Applied Surface Science 265 (2013) 720–730

Contents lists available at SciVerse ScienceDirect

Applied Surface Science

journal homepage: www.elsevier.com/locate/apsusc

Insights into the preference of $CH_x(x = 1–3)$ formation from CO hydrogenation on Cu(111) surface

Xuancheng Sun, Riguang Zhang, Baojun Wang*

Key Laboratory of Coal Science and Technology of Ministry of Education and Shanxi Province, Taiyuan University of Technology, Taiyuan 030024, Shanxi, People's Republic of China

ARTICLE INFO

Article history:
Received 25 August 2012
Received in revised form
12 November 2012
Accepted 17 November 2012
Available online 23 November 2012

Keywords:
CO
Hydrogenation
CH_x
CH_3OH
Cu(111)
Density functional theory

ABSTRACT

The mechanisms of $CH_x(x = 1\text{-}3)$ formation from CO hydrogenation on Cu(111) surface have been systematically investigated using periodic density functional calculations. The activation barriers and reaction energies for all the elementary steps involved in $CH_x(x = 1\text{-}3)$ formation is presented here. CO hydrogenation and its dissociation have been discussed. Our results show that the CO dissociation route is less energetically favored on Cu(111) surface than CO hydrogenation to form CHO and COH, in which CO mainly goes through hydrogenation to form CHO, meanwhile, the formation of CHO is more favorable both kinetically and thermodynamically than that of COH. Starting from CHO, we further investigate the formation of $CH_x(x = 1\text{-}3)$, two conditions, without H-assisted and with H-assisted, are considered. As a result, we seek out the optimal paths of $CH_x(x = 1\text{-}3)$ formation and the corresponding activation barrier of rate-controlled step on Cu(111) surface, moreover, among all $CH_x(x = 1\text{-}3)$ species, CH_2 and CH_3 are the most favored monomer for CO hydrogenation on Cu(111). In addition, our results show that CH_3OH is also easily formed by CO hydrogenation, and the formations of CH_2, CH_3 and CH_3OH by CO hydrogenation compete with each other on Cu(111) surface.

1. Introduction

Recently, syngas has been extensively used to synthesis methanol and ethanol [1–6]. Cu-based catalysts exhibits high catalytic activity to methanol synthesis from syngas [7–9]; meanwhile, for ethanol synthesis from syngas, a large number of studies mainly focus on Rh-based catalysts [10–12], however, the prohibitive cost and limited supply of Rh-based catalysts restrict their ability to be used as industrial catalysts [4,6]. Thus, much less expensive Cu-based catalysts have been an attractive option, nowadays, Cu-based catalysts have been widely used and produced promising results for ethanol synthesis from syngas in the temperature range of 280-310°C at pressures of about 40-100 bar [4,13–17]. On the other hand, the studies by Hofstadt et al. [18] have suggested that metallic Cu favors the formation of a methylene (CH_2) structure by CO hydrogenation, then, CH_2 undergo chain growth by coupling of CH_3O to form a C_2 precursor, followed by hydrogenation to produce ethanol. As a result, we can conclude that although CO hydrogenation can well produce methanol on Cu-based catalysts, CO can also hydrogenate to form CH_x via the dissociation of CH_xO and CH_xOH intermediates involved in methanol synthesis. On the basis of above facts, we can obtain that a key intermediate, $CH_x(x = 1\text{-}3)$, may involve in methanol and ethanol synthesis from CO hydrogenation on Cu-based catalysts.

To the best of our knowledge, although above reported experimental studies [4,7–9,13–18] have been performed to explore the methanol and ethanol synthesis by CO hydrogenation on Cu-based catalysts, few studies have been carried out to fully understand the formation mechanism about above mentioned key intermediate, $CH_x(x = 1\text{-}3)$, at the fundamental level due to the complexity of these reactions. For $CH_x(x = 1\text{-}3)$ formation, two possibilities exist, one is that via CO hydrogenation to form CH_xO and CH_xOH species, followed by the direct dissociation into $CH_x(x = 1\text{-}3)$ in the absence or presence of hydrogen-assisted (H-assisted); the other is that via the direct dissociation of CO to form C and O, followed by C hydrogenation to form $CH_x(x = 1\text{-}3)$ species. For example, Liu et al. [10] have found that the hydrogenation of CO to formyl species (COH or HCO) is more plausible than the direct dissociation of CO, and CH_3 is the most favorable monomer among all the $CH_x(x = 1\text{-}3)$ species on Rh(111) surface. Yet, actual mechanisms for the formation of $CH_x(x = 1\text{-}3)$ species by CO hydrogenation on Cu catalysts still remain unclear: whether surface hydrocarbon species (CH_x) is produced by the direct dissociation of CO followed by hydrogenation or that is formed via the mechanism of CO dissociation with hydrogen-assisted. Among all $CH_x(x = 1\text{-}3)$ species, which is the most favored monomer?

Nowadays, experimental information is not always sufficient and accompanying theoretical calculations can be helpful to clarify some questions. Computational chemistry methodologies have

* Corresponding author at: No. 79 Yingze West Street, Taiyuan 030024, China. Tel.: +86 351 6018239; fax: +86 351 6041237.
E-mail addresses: wangbaojun@tyut.edu.cn, quantumtyut@126.com (B. Wang).

0169-4332/$ – see front matter © 2012 Elsevier B.V. All rights reserved.
http://dx.doi.org/10.1016/j.apsusc.2012.11.091

been used as a powerful tool to study the mechanism and kinetics of several typical reactions [19–28]. By means of theoretical calculation, a detailed investigation of CH_x(x = 1-3) formation on Cu catalyst at the molecular level will help us better understand the underlying mechanisms of the reactions. Unfortunately, to the best of our knowledge, few theoretical studies are carried out to systematically investigate the mechanism of CH_x(x = 1-3) formation from CO hydrogenation on Cu(111) surface.

The aim of this study is to analyze the possible reaction pathways of CH_x(x = 1-3) formation occurring on the monometallic surface of Cu(111) by carrying out periodic density functional theory slab model calculations. A large number of unique reaction pathways involving subtly different reaction intermediates and transition states are explicitly obtained, which would provide a better understanding at the molecular level about the catalytic reactivity of the Cu catalyst towards the CH_x(x = 1-3) formation from syngas, as well as the possible reactive intermediates. Further, the results of this effort are expected to qualify the activation barriers and reaction energies of elementary steps involved in the reaction pathways of CH_x(x = 1-3) formation. In addition, our calculation may be a worthwhile theoretical example for the CH_x(x = 1-3) formation on other metal surface.

2. Computational Details

2.1. Surface model

In the surface calculation, the most stable face-center-cubic(111) surface of close-packed Cu metal, fcc(111), has been employed to investigate the catalytic behavior of CH_x(x = 1-3) formation. The Cu(111) surface is cleaved from the experimental fcc crystal structure with the lattice parameter of 3.62 Å [29], and is modeled using a three atomic layers $p(3 \times 3)$ super cell with nine atoms at each layer, which has been widely used in the previous studies about the molecule adsorption and reaction mechanism on transition metal surfaces [30–34]; this corresponds to a 1/9 monolayer (ML) coverage. Meanwhile, a 15 Å vacuum slab is employed to separate the periodically repeated slabs. The bottom layer is constrained at the bulk position in order to mimic the presence of a larger number of layers in real metal particles, whereas the upper two layers together with the adsorbed species involved in CH_x(x = 1-3) formation are allowed to relax. According to Cu(111) – [3 × 3] surface morphology, as shown in Fig. 1, there are four different adsorption sites: Top, Bridge, Hcp and Fcc.

2.2. Calculation methods

Plane-wave DFT calculations with the projector-augmented wave (PAW) method [35] are carried out as implemented in the Vienna ab initio simulation package (VASP) [36–38]. The generalized gradient approximation with the Perdew-Wang exchange-correlation functional (GGA-PW91) is used [39]. The kinetic energy cutoff for a plane wave basis set is 400 eV. The Brillouin zone is sampled using a 3 × 3 × 1 Monkhorst-Pack k-point grid (11 k-points) [40] with Methfessel-Paxton smearing of 0.1 eV [41]. The relaxation of the electronic degrees of freedom is assumed to be converged, if the total energy change and the band structure energy change between two steps are both smaller than 10^{-5} eV. A forces difference between two steps less than 0.03 eV/Å is used as the criterion for convergence of ionic relaxation.

Reactions paths have been studied using climbing-image nudged elastic band method (CI-NEB) [42,43]. Transition states have been optimized using the dimer method [44,45]. The transition state structure is deemed converged when the forces acting on the atoms are all <0.05 eV/Å for the various degrees of freedom set in the calculation. The molecules in the gas phase are calculated using a 10 × 10 × 10 Å cubic unit cell.

The adsorption energy is always regarded as a measure of the strength of adsorbate-substrate adsorption. The adsorption energies E_{ads} are defined as follows:

$$E_{ads} = E_{sub} + E_{mol} - E_{mol/sub}$$

Where $E_{mol/sub}$ is the total energy of adsorbate–substrate system in the equilibrium state, E_{sub} and E_{mol} are the total energies of substrate and free adsorbate alone, respectively. With this definition, positive values of adsorption energy denote that adsorption is more stable than the corresponding substrate and free adsorbate.

For a reaction such as AB→A + B on Cu(111) surface, the reaction energy ($\triangle H$) and activation barrier (E_a) are calculated on the basis of the following formulas:

$$\Delta H = E_{(A+B)/Cu(111)} - E_{AB/Cu(111)}$$

$$E_a = E_{TS/Cu(111)} - E_{AB/Cu(111)}$$

Where $E_{(AB)/Cu(111)}$ is the total energy for the adsorbed AB, $E_{(A+B)/Cu(111)}$ is the total energy for the co-adsorbed A and B on Cu(111) surface, and $E_{TS/Cu(111)}$ is the total energy of transition state on Cu(111) surface.

3. Results and discussion

3.1. Adsorptions of reactants and possible intermediates

Adsorptions of the reactants and all possible intermediates involved in the formation of CH_x(x = 1-3) on Cu(111) surface are investigated. The most stable adsorption configurations, the corresponding adsorption energies and key geometric parameters are listed in Table 1; Fig. 2 presents these stable adsorption configurations.

3.1.1. C, H and O

C, H and O all prefer to adsorb at the fcc sites of Cu(111) surface, as shown in Figs. 2(a)-2(c), respectively. The distances between C

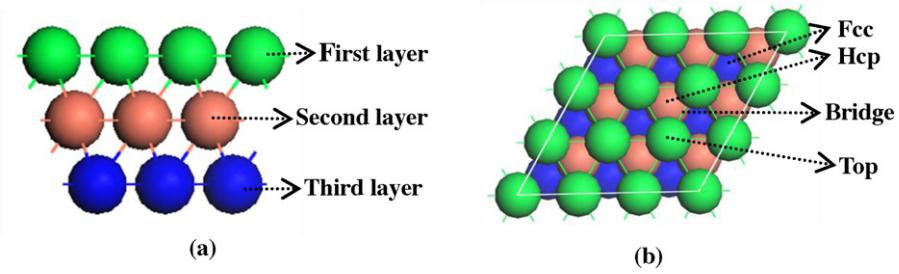

Fig. 1. The structure and adsorption sites of Cu(111) surface. (a) side view; (b) top view.

Table 1
Adsorption energies and key geometric parameters for various pertinent species involved in the formation of CH_x(x = 1-3) on Cu(111) surface.

Species	E_{ads} (kJ·mol^{-1})	Adsorption configuration	D_{Cu-X} (Å)	Bonding details	
				bond	length (Å)
C	626.4	fcc: through C	1.85	–	–
H	363.8	fcc: through H	1.74	–	–
O	669.0	fcc: through O	1.90	–	–
CO	105.5	fcc: through C	2.05	C-O	1.18
OH	377.3	fcc: through O	2.02	O-H	0.97
CH	573.2	fcc: through C	1.91	C-H	1.10
CH_2	398.9	fcc: through C	2.00/1.99/2.09	C-H	1.11/1.10
CH_3	216.6	hcp: through C	2.03/2.24/2.24	C-H	1.11
COH	363.6	fcc: through C	1.95/1.95/1.92	C-O/O-H	1.34/0.98
CH_3O	292.9	fcc: through O	2.04	C-O/C-H	1.44/1.10
CHO	191.8	fcc: C-bridge, O-top	2.07/2.07	C-O/C-H	1.28/1.11
CH_2O	33.9	fcc: C-top, O-bridge	2.05/2.07/2.06	C = O/C-H	1.36/1.10
CHOH	219.3	bridge: through C	2.02	C-H/C-O/O-H	1.10/1.36/0.99
CH_2OH	161.8	top: through C	2.02	C-H/C-O/O-H	1.10/1.46/0.98
H_2O	23.2	top: through O	2.29	O-H	0.98
CH_3OH	30.8	top: through O	2.27	C-H/C-O/O-H	1.10/1.45/0.98

atom and surface Cu atom are 1.85 Å, and the corresponding adsorption energy is found to be 626.4 kJ·mol^{-1}. The bond lengths of H – Cu and O – Cu are 1.74 and 1.90 Å, respectively, the calculated adsorption energies of H and O on Cu(111) are 363.8 and 669.0 kJ·mol^{-1}, respectively.

3.1.2. CO, OH and CH

CO, OH and CH prefer to adsorb at the fcc site of the surface, as shown in Figs. 2(d)-2(f), respectively. We can see that CO and CH tend to coordinate to the surfaces through their C atoms, respectively; OH tends to coordinate to the surface through its O atom. The adsorption energy of CO is 105.5 kJ·mol^{-1}, and the distances between the C atom and surface Cu atom are 2.02 Å. The bond length of C – O is 1.18 Å. The Cu – O and O – H bond of adsorbed OH are 2.02 and 0.97 Å, respectively, which agree well with previous DFT results with values of 2.03 and 0.97 Å on Cu(111) surface [23]. The CH is perpendicular to the surface with C – Cu and C – H bond lengths of 1.91 and 1.10 Å, respectively.

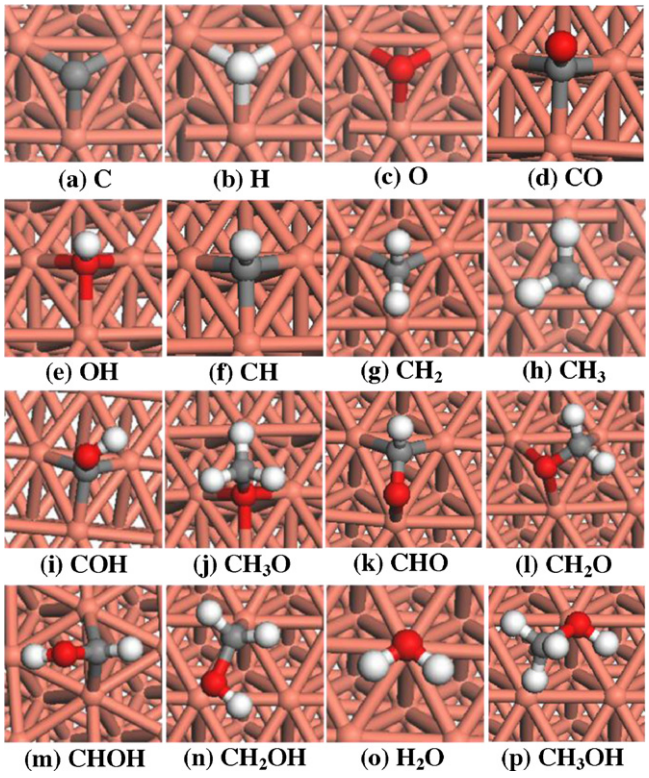

Fig. 2. The stable adsorption configurations of the reactants and all possible intermediates involved in the formation of CH_x (1-3) species on Cu(111) surface at their favorable sites. The C, O, H, and Cu atoms are shown in the grey, red, white, and orange balls, respectively.

3.1.3. CH_2 and CH_3

Unlike the high-symmetry adsorption geometries described above, the CH_2 fragment is adsorbed asymmetrically at the fcc site, as shown in Fig. 2(g). One C–H bond is elongated to 1.11 Å, with its H atom close to a Cu atom, whereas the other C–H bond points away from the surface and has a length of 1.10 Å. The adsorption energy is 398.9 kJ·mol^{-1}. CH_3 preferentially adsorbs at the hcp site through its carbon atom, as shown in Fig. 2(h). The adsorption energy is 216.6 kJ·mol^{-1}. The distances between the C atom and surface Cu atoms are 2.23, 2.24 and 2.24 Å, respectively, which agree with the previous DFT studies by Lin et al. [23].

3.1.4. COH and CH_3O

COH and CH_3O prefer to adsorb at the fcc sites of the surface, as shown in Figs. 2(i)-2(j), respectively. COH tends to coordinate to the surfaces through its C atoms; CH_3O tends to coordinate to the surface through its O atom. The O–H bond of COH is almost parallel to the surface, and the adsorption energy is 363.6 kJ·mol^{-1}. The Cu–O bond of CH_3O is perpendicular to the surface. The distances between O atom of CH_3O and surface Cu atom are 2.04 Å, and the adsorption energy is 292.9 kJ·mol^{-1}.

3.1.5. CHO and CH_2O

CHO and CH_2O prefer the top – bridge adsorption configuration on Cu (111) surfaces, as shown in Figs. 2(k)-2(l), respectively, which agree with the previous DFT results [46]. CHO binds to the surface through O anchoring at the top site and C sitting at the bridge site, which exhibits a top(O) – bridge(C) configuration with an adsorption energy of 191.8 kJ·mol^{-1}. CH_2O adsorbs on Cu(111) surface with a top(C) – bridge(O) configuration, and the corresponding adsorption energy is 33.9 kJ·mol^{-1}.

3.1.6. CHOH and CH_2OH

CHOH prefers to adsorbs at the bridge site through its C atom, as shown in Fig. 2(m). The distances between C atom and surface Cu atom are 2.02 Å. The adsorption energy is found to be 219.3 kJ·mol^{-1}. CH_2OH preferentially adsorbs at the top site through its C atom, as shown in Fig. 2(n). The C – O axis is almost parallel to the Cu(111) surface with an adsorption energy of 161.8 kJ·mol^{-1}.

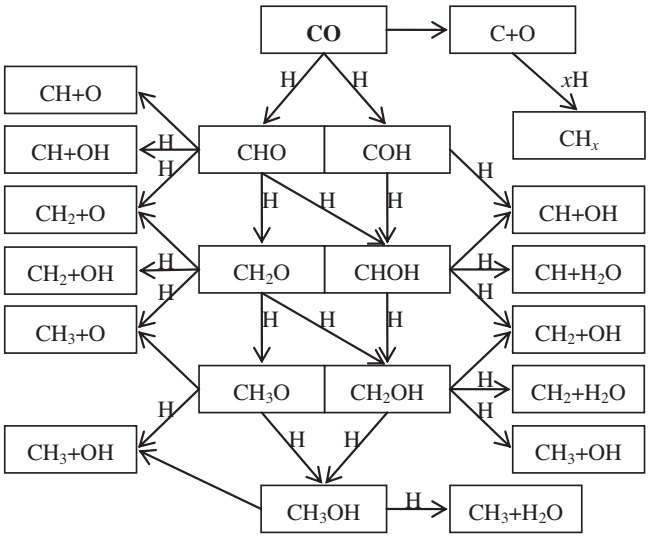

Fig. 3. Reaction network scheme of the CH_x(x = 1-3) formation by CO hydrogenation and dissociation.

3.1.7. H_2O and CH_3OH

H_2O and CH_3OH are weakly bound to the top sites of Cu(111) through their O atoms, as shown in Figs. 2(o)-2(p), respectively. The plane of adsorbed H_2O is nearly parallel to the surface with the O – Cu bond length of 2.29 Å, and the corresponding adsorption energies is 23.2 kJ·mol^{-1}. The C – O axis of adsorbed CH_3OH is tilted relative to the normal of the Cu(111) surface, which has an adsorption energy of 30.8 kJ·mol^{-1}, and the length of O – Cu bond is 2.27 Å.

3.2. Reaction network of CH_x (x = 1-3) formation by CO hydrogenation

The reaction network of CH_x(x = 1-3) formation from CO hydrogenation and dissociation on Cu(111) surface is displayed in Fig. 3. The adsorbed CO can dissociate via a series of sequential steps to form CH_x(x = 1-3). There are two possibilities for CH_x(x = 1-3) formation: one is through CO hydrogenation to form C_1 oxygenated entities, followed by the dissociation in the presence or absence of H-assisted to produce CH_x(x = 1-3); the other is via CO direct dissociation to form C and O atoms, followed by the hydrogenation of C to form CH_x(x = 1-3). Thus, we first investigate CO hydrogenation and dissociation, followed by CH_x (x = 1-3) formation. As shown in Fig. 3, a large number of reaction paths leading to CH_x (x = 1-3) formation are considered in the present DFT study, and on this basis, an optimal path for CH_x (x = 1-3) formation will be identified.

Table 2
Calculated activation barriers (E_a) and reaction energies (ΔH) of the elementary reactions for CO hydrogenation and dissociation.

Reactions	E_a (kJ·mol^{-1})	ΔH (kJ·mol^{-1})
CO + H → CHO	105.8	82.3
CO + H → COH	233.3	97.8
CO → C + O	365.5	250.4

3.2.1. CO hydrogenation and dissociation

The activation barriers and reaction energies for CO hydrogenation and dissociation on Cu(111) surface are listed in Table 2. The geometries of the initial states (IS), transition states (TS) and final states (FS) are displayed in Fig. 4.

For CO hydrogenation, there are two possibilities, one with H attacking at C center of CO to produce CHO, and the other with H attacking at O center of CO to form COH. For CHO formation, starting from IS1, CO adsorbs at the fcc site, H locates at the adjacent fcc site, both are the most stable configuration of CO and H species on Cu(111) surface, respectively. H adatom is transferred from the fcc site in IS1 to the C atom of CO in FS1 through the transition state TS1. In TS1, the distance between H and C is decreased to 1.14 Å from 2.81 Å in IS1. The activation barrier for this elementary reaction is 105.8 kJ·mol^{-1}, and the reaction is found to be endothermic by 82.3 kJ·mol^{-1}. While for COH formation, beginning with IS1, H adatom is transferred from the fcc site in IS1 to the O atom of CO in FS2 through a transition state TS2. In TS2, the distances between H and O atoms is decreased to 1.31 Å from 3.26 Å in IS1. This elementary reaction is endothermic by 97.8 kJ·mol^{-1}, with a large activation barrier of 233.3 kJ·mol^{-1}. Grabow et al. [29] have investigated CO hydrogenation to CHO and COH on Cu(111) surface, which show that the activation barrier are 95.5 and 224.8 kJ·mol^{-1}, respectively, those values are close to our results.

On the other hand, for CO direct dissociation, starting from IS3, with the C – O bond activation of CO through the transition state TS3. The distance between C and O atoms is elongated from 1.18 Å in IS3 to 2.05 Å in TS3, and 3.77 Å in FS3. This elementary reaction is endothermic by 250.4 kJ·mol^{-1}, with a significantly large activation barrier of 365.5 kJ·mol^{-1} in comparison with those of the CO hydrogenation.

On the basis of above results, we can obtain that when CO and H is co-adsorbed on Cu(111) surface, Cu(111) surface show rather low catalytic activity for CO direct dissociation, CO dominantly hydrogenate to form CHO both kinetically and thermodynamically than COH formation and CO direct dissociation, indicating that CHO is the dominant product for CO hydrogenation on Cu(111) surface.

3.2.2. CH formation

As mentioned above, CO hydrogenation to form CHO is the dominant product for CO hydrogenation on Cu(111) surface, as a result,

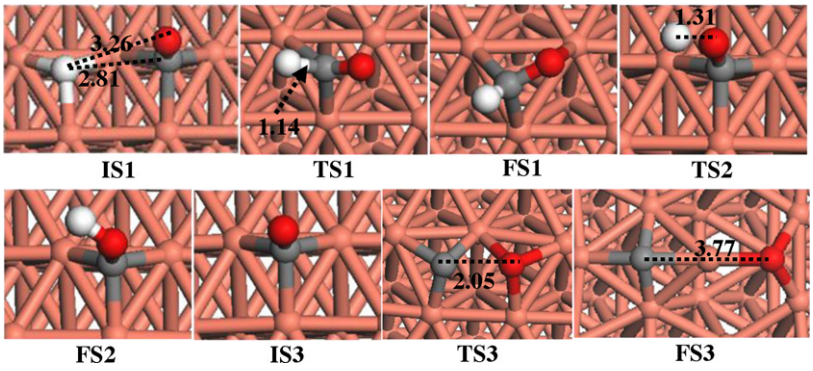

Fig. 4. The initial states (IS), transition states (TS) and final states (FS) for CO hydrogenation and dissociation reactions. Bond lengths are in Å. See Fig. 2 for color coding.

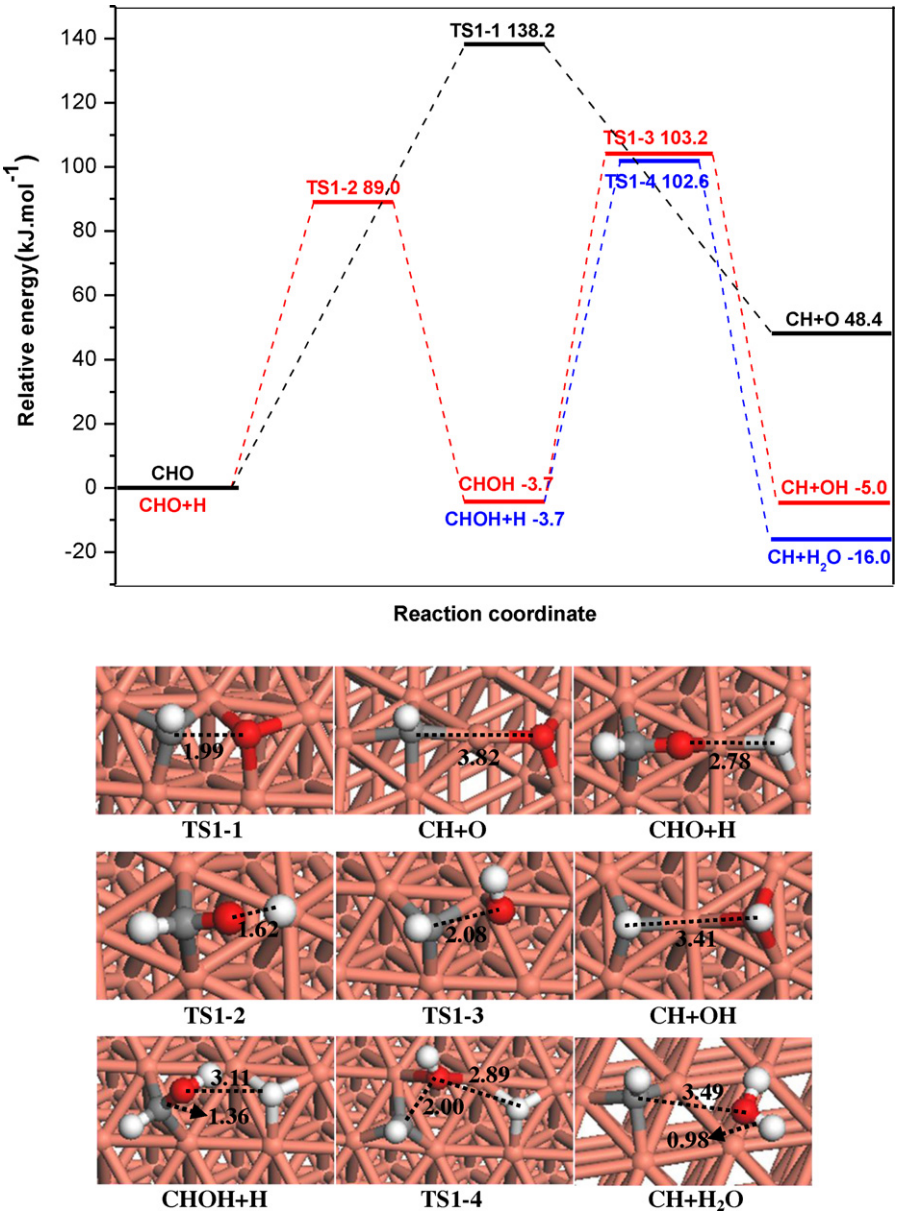

Fig. 5. The potential energy diagram for CH formation in together with the structures of partial initial states, transition states and final states. Bond lengths are in Å. See Fig. 2 for color coding.

in this study, we only consider the formation of CH_x(x = 1-3) starting from CHO. As shown in Fig. 3, there are two possibilities for CH formation; one is the direct dissociation of CHO or CHOH without H-assisted, the other is the indirect dissociation of CHO or CHOH with H-assisted. The potential energy diagram for these reactions of CH formation in together with the initial states, transition states and final states are illustrated in Figs. 2 and 5, respectively.

3.2.2.1. (A) CH formation without H-assisted. Two possible paths for the formation of CH without H-assisted are discussed, in which Path 1-1 is the CH formation through the C – O bond scission of CHO, and Path 1-2 is the formation of CH via CHO hydrogenation to form CHOH, followed by its C – O bond scission.

In Path 1-1, starting from CHO (Fig. 2), the C – O bond cleavage of CHO can lead to the formation of CH and O through a transition state TS1-1 (Fig. 5). The distance between C and O atoms is elongated from 1.28 Å in CHO to 1.99 Å in TS1-1, and 3.82 Å in CH + O. This elementary reaction is found to be endothermic by 48.4 kJ·mol^{-1}, with an activation barrier of 138.2 kJ·mol^{-1}.

In Path 1-2, beginning with CHO + H (Fig. 5), the H adatom approaches the O atom of adsorbed CHO to form CHOH (Fig. 2) through the transition state TS1-2. In TS1-2, the distance between H and O atoms is decreased to 1.62 Å from 2.78 Å in CHO + H. The activation barrier for this elementary reaction is 89.0 kJ·mol^{-1}, and this reaction is found to be exothermic by 3.7 kJ·mol^{-1}. Then, the C – O bond cleavage of CHOH can form the co-adsorbed CH and OH through a transition state TS1-3. In CH + OH, CH locates at the fcc site, OH sits at the hcp site. In this step, the main component of the reaction coordinate is the elongation of C – O bond; this bond is extended to 2.08 Å in TS1-3, 3.41 Å in CH + OH from 1.36 Å in CHOH equilibrium bond length. The activation barrier for this elementary reaction is 106.9 kJ·mol^{-1}, and the reaction is found to be slightly exothermic by 1.3 kJ·mol^{-1}. So the rate-controlled step for Path 1-2 occurs at TS1-3 with an activation barrier of 106.9 kJ·mol^{-1}.

3.2.2.2. (B) CH formation with H-assisted. For the formation of CH with H-assisted, two possible paths are still considered, one is Path 1-3 with the formation of CH through C – O bond scission of CHO with H-assisted, and the other is Path 1-4 with the formation of CH via CHO hydrogenation to form CHOH, followed by the C – O bond scission with H-assisted.

In Path 1-3, we use the dimer approach to search for the transition state of the C – O bond scission of CHO with H-assisted, interestingly, the obtained TS is similar to the TS of CHO hydrogenation to form CHOH. As a result, the dissociation of CHO with H-assisted prefers to be hydrogenated to form CHOH rather than producing CH and OH.

In Path 1-4, as described in Path 1-2, CHO first hydrogenate to form CHOH. Thus, we only discuss the dissociation of CHOH with H-assisted to form CH and H_2O. Starting from CHOH + H, in which CHOH adsorbs at the bridge site, H locates at the fcc site, both are the most stable configuration of CHOH and H species on Cu(111) surface, respectively; the C – O bond cleavage of CHOH with H-assisted leads to CH and H_2O through a transition state TS1-4. The distance between C and O atoms is elongated to 2.00 Å in TS1-4, 3.49 Å in CH + H_2O from 1.36 Å in CHOH + H, and the distance between H and O is decreased to 2.89 Å in TS1-4, 0.98 Å in CH + H_2O from 3.11 Å in CHOH + H, respectively. In CH + H_2O, CH binds at the hcp site, H_2O is far away the surface, and its molecular plane is nearly parallel to Cu(111) surface. The activation barrier and reaction energy for this step are 106.3 and -12.3 kJ·mol^{-1}. So the rate-controlled step for Path 1-4 occurs at TS1-4 with an activation barrier of 106.3 kJ·mol^{-1}.

3.2.2.3. (C) The comparisons of activation barriers in Paths 1-1,1-2,1-4. A summary potential energy diagram for the formation of CH from CHO hydrogenation on Cu(111) surface is shown in Fig. 5. The rate-controlled step for Paths 1-1, 1-2 and 1-4 occur at TS1-1, TS1-3 and TS1-4, respectively, the corresponding activation barriers are 138.2, 106.9 and 106.3 kJ·mol^{-1} with the reaction energies of 48.4, -1.3 and -12.3 kJ·mol^{-1}, respectively, which suggests that the activation barriers of rate-controlled step for Path 1-2 and Path 1-4 are nearly close, while for Path 1-1 has a larger activation barrier of rate-controlled step. Thus, Path 1-2 (CHO + H→CHOH→CH + OH) and Path 1-4 (CHO + H→ CHOH + H→CH + H_2O) are two parallel paths, which areresponsible for CH formation from CHO hydrogenation on Cu(111) surface.

3.2.3. CH_2 formation

As shown in Fig. 3, there are still two possibilities for the formation of CH_2; one is the direct dissociation of CH_2O or CH_2OH without H-assisted, the other is the indirect dissociation of CHO, CH_2O, CHOH and CH_2OH with H-assisted. The potential energy diagram for these reactions of CH_2 formation in together with the initial states, transition states, final states are displayed in Figs. 2 and 6, respectively.

3.2.3.1. (A) CH_2 formation without H-assisted. There are three possible paths for the formation of CH_2 without H-assisted, in which Path 2-1 is the formation of CH_2 via CHO hydrogenation to form CH_2O, followed by the C – O bond scission of CH_2O; Path 2-2 is the formation of CH_2 via CHO hydrogenation to form CHOH, followed by hydrogenation to form CH_2OH, after that, the C – O bond scission of CH_2OH to form CH_2 and OH; Path 2-3 is the formation of CH_2 via CHO hydrogenation to form CH_2O, followed by hydrogenation to form CH_2OH, after that, the C – O bond scission of CH_2OH to form CH_2 and OH.

In Path 2-1, starting from CHO + H, as shown in Fig. 6, with the H adatom approaching the adsorbed CHO, CHO can hydrogenate via the transition state TS2-1 to form CH_2O (Fig. 2). In TS2-1, the distance between H adatom and C is decreased to 1.65 Å from 2.81 Å in CHO + H. The activation barrier of this elementary reaction is 49.7 kJ·mol^{-1}, and the reaction is found to be exothermic by 22.4 kJ·mol^{-1}. Subsequently, the C – O bond cleavage of CH_2O can form CH_2 and O through a transition state TS2-2. The distance between H adatom and C is extended to 2.00 Å in TS2-2 and 3.76 Å in CH_2 + O from 1.36 Å in CH_2O. The activation barrier of this elementary reaction is 111.0 kJ·mol^{-1} and the reaction is found to be endothermic by 29.4 kJ·mol^{-1}.

In Path 2-2, as described in Path 1-2, CHO first hydrogenate to form CHOH, then, beginning with CHOH + H, with the H atom approaching the adsorbed CHOH, CHOH can hydrogenate via the transition state TS2-3 to form CH_2OH. The distance between H adatom and C is decreased from 3.03 Å in CHOH + H to 1.69 Å in TS2-3. The activation barrier of this elementary reaction is 42.4 kJ·mol^{-1} and the reaction is found to be exothermic by 28.2 kJ·mol^{-1}, subsequently, the C – O bond cleavage of CH_2OH can lead to the formation of CH_2 and OH through a transition state TS2-5. The distance between C and O is elongated from 1.46 Å in CH_2OH to 1.97 Å in TS2-5 and 3.06 Å in CH_2 + OH. This step is found to be exothermic by 19.4 kJ·mol^{-1}, with an activation barrier of 84.8 kJ·mol^{-1}.

In Path 2-3, as described in Path 2-1, CHO first hydrogenate to form CH_2O, then, beginning with CH_2O + H, the O atom of CH_2O can interact with the H adatom to product CH_2OH via the transition state TS2-4. In TS2-4, the distance between H adatom and C is shortened to 1.46 Å from 2.90 Å in CH_2O + H. The activation barrier of this elementary reaction is 89.4 kJ·mol^{-1}, and the reaction is found to be slightly endothermic by 3.4 kJ·mol^{-1}. Further, the decomposition of CH_2OH is the same with that described in Path 2-2.

3.2.3.2. (B) CH_2 formation with H-assisted. Five possible paths are considered to form CH_2 with H-assisted, Path 2-4 is the first one via the C – O bond scission of CHO with H-assisted to form CH_2 and O; Path 2-5 is that via CHO hydrogenation to form CH_2O, followed by the C – O bond scission with H-assisted to form CH_2 and OH; Path 2-6 is that via CHO hydrogenation to form CHOH, followed by the C – O bond scission with H-assisted to form CH_2 and OH; Path 2-7 is that via Path 2-2 to form CH_2OH, followed by the C – O bond scission of CH_2OH with H-assisted to form CH_2 and H_2O; finally, Path 2-8 is that via Path 2-3 to form CH_2OH, followed by the C – O bond scission of CH_2OH with H-assisted to form CH_2 and H_2O.

In Path 2-4, interestingly, an intermediate between reactant and product is found to be similar to the absorbed CH_2O, suggesting that the dissociation of CHO with H-assisted first form CH_2O, not produce CH_2 and O.

In Path 2-5, as described in Path 2-1, CHO first hydrogenate to form CH_2O. Then, we search for the transition state of the C – O bond scission of CH_2O with H-assisted to form CH_2 and OH, however, the obtained TS is similar to that of CH_2O hydrogenation to form CH_2OH. Thus, the dissociation of CH_2O with H-assisted prefers to be hydrogenated to form CH_2OH, not produce CH_2 and OH.

In Path 2-6, similarly, as described in Path 1-2, CHO first hydrogenate to form CHOH. Then, an intermediate for the C – O bond scission of CHOH with H-assisted to form CH_2 and OH is similar to the absorbed CH_2OH; indicating that the dissociation of CHOH with H-assisted prefers to be hydrogenated to form CH_2OH, not produce CH_2 and OH.

In Path 2-7 and Path 2-8, as described in Path 2-2 and Path 2-3, respectively, CHO first hydrogenate to form CH_2OH, subsequently, starting from CH_2OH + H, in which CH_2OH and H are adsorbed at the top and fcc site, respectively, the C – O bond cleavage of CH_2OH with H-assisted can form CH_2 and H_2O through a transition state TS2-6. The distance between C and O atoms is elongated from 1.41 Å in CH_2OH + H to 3.35 Å in TS2-6, 3.49 Å in CH_2 + H_2O, and the distance between H adatom and O is decreased from 3.33 Å in CH_2OH + H to 1.59 Å in TS2-6, 0.98 Å in CH_2 + H_2O, respectively. In

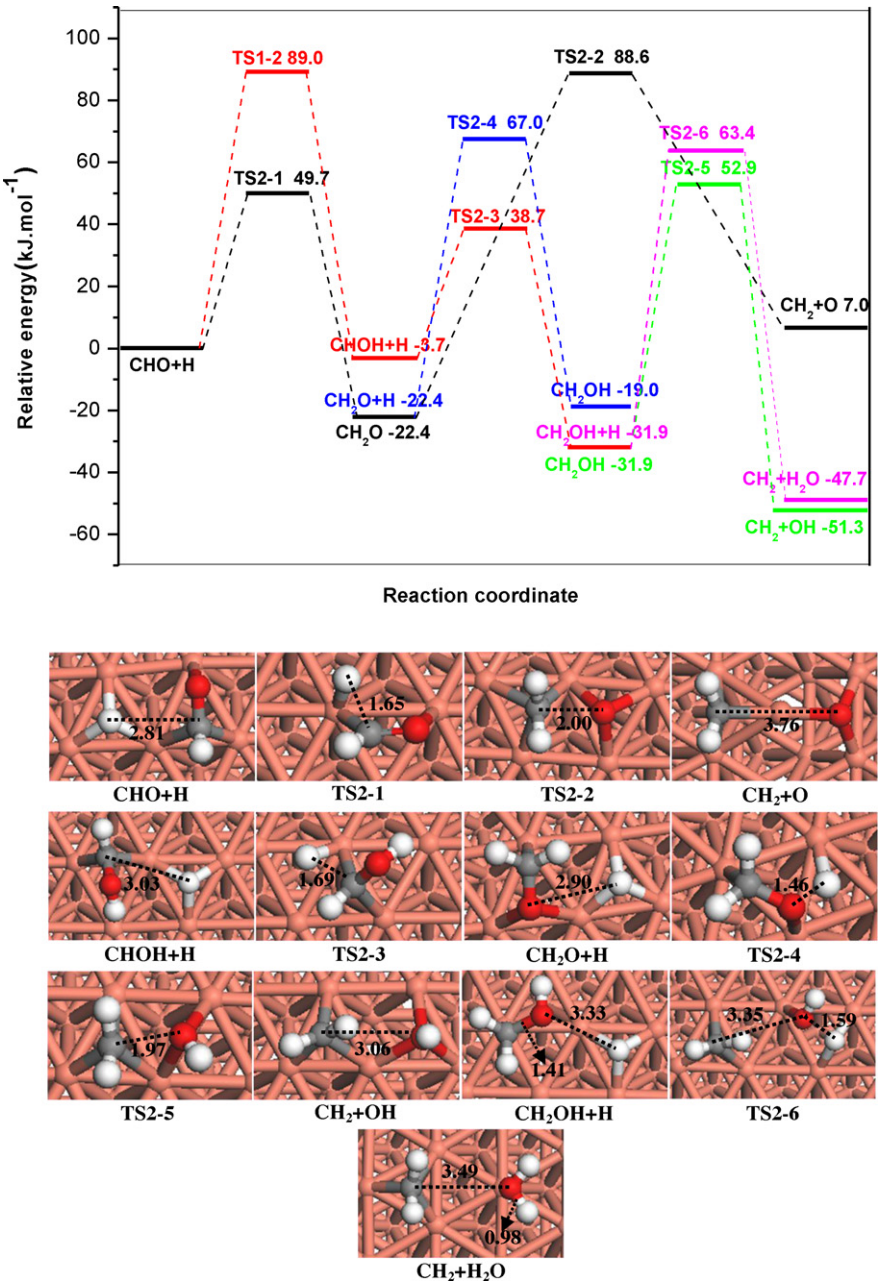

Fig. 6. The potential energy diagram for CH_2 formation in together with the structures of partial initial states, transition states and final states. Bond lengths are in Å. See Fig. 2 for color coding.

$CH_2 + H_2O$, CH_2 adsorbs at the hcp site, H_2O is far away the surface, and its molecular plane is parallel to the Cu(111) surface. This elementary reaction is found to be exothermic by 15.8 kJ·mol^{-1}, with an activation barrier of 95.3 kJ·mol^{-1}.

3.2.3.3. (C) The comparisons of activation barriers in Paths 2-(1∼3) and 2-(7∼8). On the basis of above results, we can see that Paths 2-(1∼3) and 2-(7∼8) are responsible for the formation of CH_2. Fig. 6 presents a summary potential energy diagram of these paths for the formation of CH_2 with respect to CHO + H on Cu(111) surface. The rate-controlled step for Paths 2-1, 2-2, 2-3, 2-7 and 2-8 occurs at TS2-2, TS1-2, TS2-4, TS2-6 and TS2-6, respectively, the corresponding activation barriers are 111.0, 89.0, 89.4, 95.3 and 95.3 kJ·mol^{-1} with the reaction energies of 29.4, -3.7, 3.4, -15.8 and -15.8, respectively. As a result, for the Paths 2-2, 2-3, 2-7 and 2-8, the activation barriers of rate-controlled step only have a little difference, which is smaller than 6.3 kJ·mol^{-1}, while for Path 2-1, it has a larger activation barrier of rate-controlled step. Thus, Path 2-2 (CHO + H→CHOH + H→CH_2OH→CH_2 + OH), Path 2-3 (CHO + H→CH_2O +H→CH_2OH→CH_2 + OH), Path 2-7 (CHO + H→CHOH + H→CH_2OH +H→CH_2 + H_2O) and Path 2-8 (CHO + H→CH_2O + H→CH_2OH + H→CH_2 + H_2O) are thought to be four parallel paths, which are mainly responsible for CH_2 formation from CHO hydrogenation on Cu(111) surface.

3.2.4. CH_3 formation

As shown in Fig. 3, there are two possibilities for the formation of CH_3; one is the direct dissociation of CH_3O or CH_3OH without H-assisted, the other is the indirect dissociation of CH_2O, CH_3O, CH_2OH or CH_3OH with H-assisted. The potential energy diagram for these reactions of CH_3 formation in together with the initial

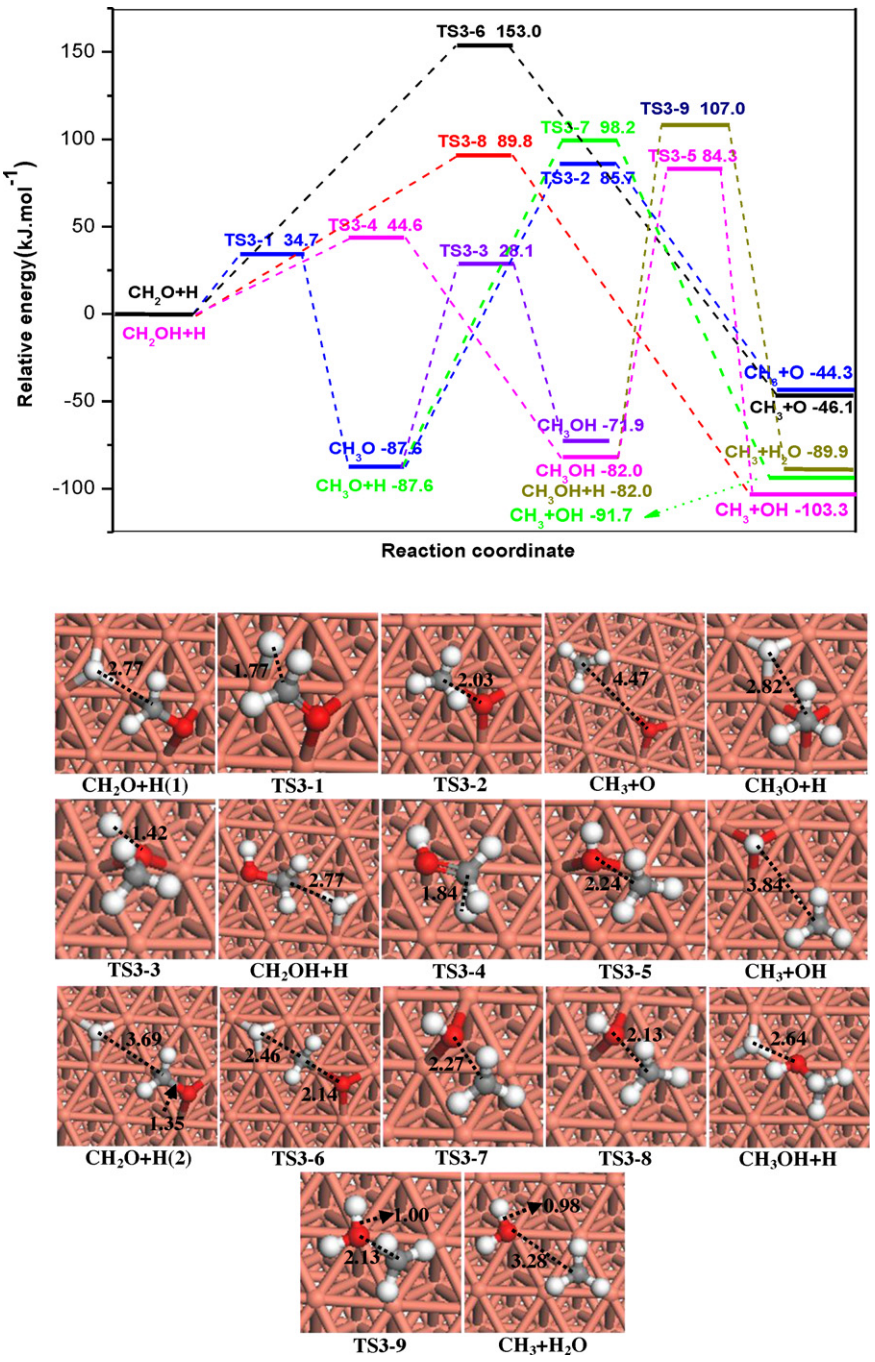

Fig. 7. The potential energy diagram for CH_3 formation in together with the structures of partial initial states, transition states and final states. Bond lengths are in Å. See Fig. 2 for color coding.

states, transition states and final states are displayed in Figs. 2 and 7, respectively.

3.2.4.1. (A) CH_3 formation without H-assisted. Four possible paths for the formation of CH_3 without H-assisted exist, Path 3-1 is the formation of CH_3 via CHO hydrogenation to form CH_3O, followed by its C – O bond scission; Path 3-2 is that via CHO hydrogenation to form CH_3O, followed by hydrogenation to form CH_3OH, after that, the C – O bond scission of CH_3OH to form CH_3 and OH; Path 3-3 is that via Path 2-2 to form CH_2OH, followed by hydrogenation to form CH_3OH, after that, the C – O bond scission of CH_3OH to form CH_3 and OH; Path 3-4 is that via Path 2-3 to form CH_2OH, followed by hydrogenation to form CH_3OH, then, the C – O bond scission of CH_3OH to form CH_3 and OH.

In Path 3-1, as described in Path 2-1, CHO first hydrogenate to form CH_2O. Then, the hydrogenation of CH_2O leads to the formation of CH_3O via the transition state TS3-1; subsequently, the C – O bond scission of CH_3O results in CH_3 and O via a transition state TS3-2. Beginning with CH_2O + H(1) to form CH_3O, in TS3-1, the distance between H adatom and C is decreased to 1.77 Å from 2.77 Å in CH_2O + H. The activation barrier of this elementary reaction is 34.7 kJ·mol^{-1} and the reaction is found to be exothermic by 87.6 kJ·mol^{-1}. Then, the C – O bond cleavage of CH_3O (Fig. 2) can form CH_3 and O, the distance between O and C atoms is elongated to 2.03 Å TS3-2 and 4.47 Å in CH_3 + O from 1.44 Å in CH_3O. In CH_3 + O,

CH_3 adsorbs at the hcp site, O locates at the fcc site, both are the most stable configuration of CH_3 and O species on Cu(111) surface. The activation barrier of this elementary reaction is 173.3 kJ·mol^{-1} and the reaction is found to be endothermic by 43.3 kJ·mol^{-1}.

In Path 3-2, as described in Path 3-1, CHO first hydrogenate to form CH_3O. Then, CH_3O hydrogenates to form CH_3OH, followed by the C – O bond scission of CH_3OH to form CH_3 and OH. Starting from CH_3O + H, CH_3O adsorbs at the fcc site, H adsorbs at the fcc site, both are the most stable configuration of CH_3O and H species on Cu(111) surface, respectively. The H adatom is transferred from the fcc site in CH_3O + H to the O atom of CH_3O through the transition state TS3-3. In TS3-3, the distance between H adatom and C is decreased to 1.42 Å from 2.82 Å in CH_3O + H. The activation barrier for CH_3O hydrogenation to CH_3OH is 115.7 kJ·mol^{-1}, and the reaction is found to be endothermic by 15.7 kJ·mol^{-1}. For CH_3OH decomposition, beginning with CH_3OH (Fig. 2), the C – O bond cleavage can lead to the formation of CH_3 and OH through a transition state TS3-5. The distance between C and O atoms is elongated from 1.45 Å in CH_3OH to 2.24 Å in TS3-5 and 3.84 Å in CH_3 + OH. In CH_3 + OH, CH_3 adsorbs at the hcp site, OH sits at the fcc site, both are the most stable configuration of CH_3 and OH species on Cu(111) surface. This elementary step is found to be exothermic by 21.3 kJ·mol^{-1}, with an activation barrier of 166.3 kJ·mol^{-1}.

In Paths 3-3 and 3-4, as described in Paths 2-2 and 2-3, respectively, CHO first hydrogenate to form CH_2OH. Then, the hydrogenation of CH_2OH is to form CH_3OH via the transition state TS3-4. In TS3-4, the distance between H and C is decreased to 1.84 Å from 2.77 Å in CH_2OH + H. The activation barrier of this elementary reaction is 44.6 kJ·mol^{-1} and the reaction is found to be exothermic by 82.0 kJ·mol^{-1}. Finally, the C – O bond scission of CH_3OH without H-assisted to form CH_3 and OH is the same as described in Path 3-2.

3.2.4.2. (B) CH_3 formation with H-assisted. For the formation of CH_3 with H-assisted, seven possible paths are considered, Path 3-5 is that via CHO hydrogenation to form CH_2O, followed by the C – O bond scission of CH_2O with H-assisted form CH_3 and O; Path 3-6 is that via CHO hydrogenation to form CH_3O, followed by the C – O bond scission of CH_3O with H-assisted form CH_3 and OH; Path 3-7 is that via Path 2-2 to form CH_2OH, followed by the C – O bond scission of CH_2OH with H-assisted to form CH_3 and OH; Path 3-8 is that via Path 2-3 to form CH_2OH, followed by the C – O bond scission of CH_2OH with H-assisted to form CH_3 and OH; Path 3-9 is the formation of CH_3 via Path 3-2 to form CH_3OH, followed by the C – O bond scission of CH_3OH with H-assisted to form CH_3 and H_2O; Path 3-10 is that via Path 3-3 to form CH_3OH, followed by the C – O bond scission of CH_3OH with H-assisted to form CH_3 and H_2O. Finally, Path 3-11 is that via Path 3-4 to form CH_3OH, followed by the C – O bond scission of CH_3OH with H-assisted to form CH_3 and H_2O.

In Path 3-5, as described in Path 2-1, CHO first hydrogenate to form CH_2O. Then, the C – O bond scission of CH_2O with H-assisted to form CH_3 and O. Starting from CH_2O + H(2), CH_2O adsorbs at the top(C)-bridge(O) site, H sits at the fcc site. The C – O bond scission of CH_2O with H-assisted goes through a transition state TS3-6, in which the distance between H adatom and C decreases to 2.46 Å from 3.69 Å in CH_2O + H(2), and the distance between C and O atoms is extended to 2.14 Å from 1.35 Å in CH_2O + H(2). This elementary step is found to be exothermic by 46.1 kJ·mol^{-1}, with an activation barrier of 153.0 kJ·mol^{-1}.

In Path 3-6, as described in Path 3-1, CHO first hydrogenate to form CH_3O, subsequently, the C – O bond scission of CH_3O with H-assisted leads to CH_3 and OH via a transition state TS3-7. In TS3-7, the distance between C and O atoms is 2.27 Å. This step is found to be slightly exothermic by 4.1 kJ·mol^{-1}, and with an activation barrier of 185.8 kJ·mol^{-1}.

In Paths 3-7 and 3-8, as described in Paths 2-2 and 2-3, respectively, CHO first hydrogenate to form CH_2OH, subsequently, the C – O bond scission of CH_2OH with H-assisted can form CH_3 and OH via a transition state TS3-8. This elementary step is found to be exothermic by 103.3 kJ·mol^{-1}, and with an activation barrier of 89.8 kJ·mol^{-1}.

In Paths 3-9, 3-10 and 3-11, as described in Paths 3-2, 3-3 and 3-4, respectively, CHO sequentially hydrogenate to form CH_3OH. Then, the C – O bond scission of CH_3OH with H-assisted leads to the formation of CH_3 and H_2O via a transition state TS3-9, starting from CH_3OH + H, in which CH_3OH adsorbs at the top site, H adsorbs at the hcp site. The distance between H adatom and O is decreased from 2.64 Å in CH_3OH + H to 1.00 Å in TS3-9 and 0.98 Å in CH_3 + H_2O, and the distance between C and O atoms is extended from 1.44 Å in CH_3OH + H to 2.13 Å in TS3-9 and 3.28 Å in CH_3 + H_2O. In CH_3 + H_2O, CH_3 adsorbs at the hcp site, H_2O adsorbs at the top site, and its molecular plane is parallel to the Cu(111) surface, both are the most stable configuration of CH_3 and H_2O species on Cu(111) surface, respectively. This elementary step is found to be slightly exothermic by 7.9 kJ·mol^{-1}, with an activation barrier of 189.0 kJ·mol^{-1}.

3.2.4.3. (C) The comparisons of activation barriers in Paths 3-(1∼11). Following the summary potential energy diagram for CH_3 formation from CHO hydrogenation on Cu(111) surface, as shown in Figs. 6 and 7, respectively, we can see that the rate-controlled step for Paths 3-(1∼11) occur at TS3-2, TS3-5, TS3-5, TS3-5, TS3-6, TS3-7, TS3-8, TS3-8, TS3-9, TS3-9 and TS3-9, respectively, the corresponding activation barriers are 173.3, 166.3, 166.3, 166.3, 153.0, 185.8, 89.8, 89.8, 189.0, 189.0 and 189.0 kJ·mol^{-1} with the reaction energies of 43.3, -21.3, -21.3, -21.3, -46.1, -4.1,-103.3, -103.3, -7.9, -7.9 and -7.9, respectively. As a result, Paths 3-7 and 3-8 have the same rate-controlled step via TS3-8, and have smaller activation barrier and reaction energy than other paths. Thus, Path 3-7 (CHO + H→CHOH + H→ CH_2OH + H→CH_3 + OH) and Path 3-8 (CHO + H→CH_2O + H→CH_2OH + H→CH_3 + OH) are two parallel and dominant paths contributing to CH_3 formation, which are more favorable both kinetically and thermodynamically than other paths.

3.3. General discussion

In this study, we have investigated two possibilities for the reaction of CO: one is CO hydrogenation to form CHO and COH species; the other is CO direct dissociation into C and O. Our results show that the hydrogenation of CO to form CHO is more favorable both kinetically and thermodynamically than the dissociation of CO and the formation of COH. As a result, it is concluded that the adsorbed CO species dominantly undergoes the hydrogenation to form CHO on Cu(111) surface.

On the basis of above results, starting from CHO and CHO hydrogenation, CH_x(x = 1-3) formation without H-assisted and with H-assisted are systematically investigated, respectively. The optimal paths for CH_x(x = 1-3) formation starting from CHO, as well as the corresponding activation barriers and reaction energies on Cu(111) surface are presented in Fig. 8. For CH formation among four paths, Paths 1-2 and 1-4 are two parallel and dominant paths to form CH on Cu(111) surface, and the corresponding activation barriers of rate-controlled step are 106.9 and 106.3 kJ·mol^{-1}, respectively. For CH_2 formation, eight paths are considered, four parallel paths, Paths 2-2, 2-3, 2-6 and 2-7, are mainly responsible for CH_2 formation on Cu(111) surface, and the corresponding activation barriers of rate-controlled step are 89.0, 89.4, 95.3 and 95.3 kJ·mol^{-1}, respectively. For CH_3 formation, two parallel paths, Paths 3-7 and 3-8, are responsible for CH_3 formation on Cu(111) surface, and the corresponding activation barriers of rate-controlled step are 89.8 and 89.8 kJ·mol^{-1}, respectively. As a result, among all

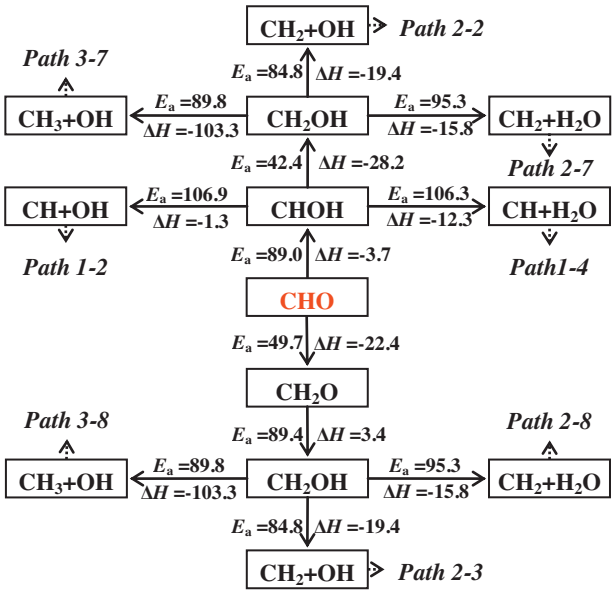

Fig. 8. The optimal paths for the formation of CH_x(x = 1-3) starting from CHO on Cu (111) surface, as well as the corresponding activation barriers and reaction energies of every elementary step.

CH_x(x = 1-3) species, CH_2 and CH_3 are the most favored monomer on the basis of activation barriers.

On the other hand, considering the high catalytic activity of Cu-based catalysts for methanol synthesis from syngas, we further investigate the formation mechanism of CH_3OH from CO hydrogenation, as shown in Fig. 3, three pathways are responsible for CH_3OH formation, Fig. 9 presents the summary potential energy diagram for CH_3OH formation starting from CHO hydrogenation on Cu(111) surface. We can see that the corresponding rate-controlled steps of these three pathways CHO + H→CHOH + H→CH_2OH + H→CH_3OH, CHO + H→CH_2O + H→CH_2OH +H→CH_3OH, and CHO + H→CH_2O + H→CH_3O + H→CH_3OH occur at TS1-2, TS2-4 and TS3-3, respectively, the corresponding activation barriers are 89.0, 89.4 and 115.7 kJ·mol^{-1} with the reaction energies of -3.7, 3.4 and 15.7 kJ·mol^{-1}, respectively, suggesting that the pathways of CHO + H→CHOH + H→ CH_2OH + H→CH_3OH and CHO + H→CH_2O + H→CH_2OH + H→CH_3OH are more favorable for CH_3OH formation among three pathways. As a result, we can obtain that for CO hydrogenation on Cu(111) surface, the formation

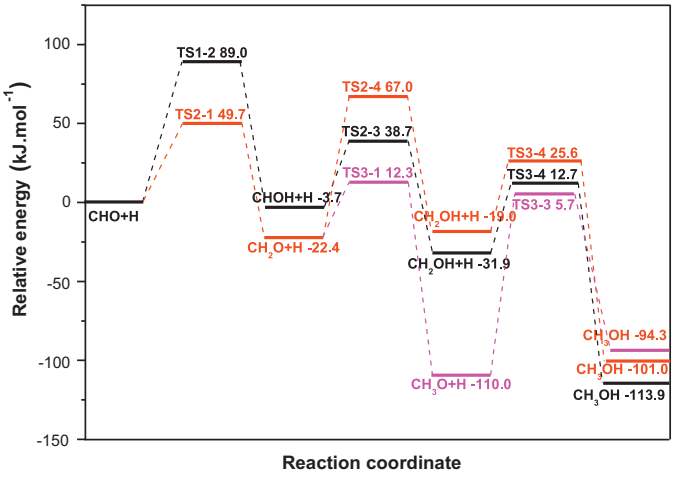

Fig. 9. The potential energy diagram for CH_3OH formation from CHO hydrogenation on Cu(111) surface.

of CH_2, CH_3 and CH_3OH are three parallel reactions in dynamics, and compete with each other, indicating that CH_3OH formation may reduce the production of CH_2 and CH_3.

In addition, previous studies by An et al. [47] have investigated the effect of Cu added into Ni on the steam reforming of CH_4, their results show that that the activation barrier of the dehydrogenation of CH_x(x = 1-4) and the hydrogenation of CH_x(x = 0-3) on Cu/Ni(111) surface are larger than that on pure Ni(111) surface, suggesting that the added Cu into Ni can hinder CH_4 formation by CH_x(x = 0-3) hydrogenation, as a result, Cu-based catalysts may be inertia for catalyzing CH_2 and CH_3 hydrogenation to form CH_4, which may be in favor of the methanol and ethanol synthesis.

4. Conclusions

In this study, density functional theory method is employed to fully investigate the formation of CH_x(x = 1-3) from CO hydrogenation on Cu(111) surface. CO hydrogenation and dissociation have been discussed. Our results show that CO mainly hydrogenate to form CHO, in which CHO formation is supported both kinetically and thermodynamically than that of COH, meanwhile, the CO dissociation route is not energetically favored on Cu(111) surface.

Based on the above result, we further investigate the formation of CH_x(x = 1-3) starting from CHO, two conditions, without H-assisted and with H-assisted, are considered. We obtain the optimal paths of CH_x(x = 1-3) formation and the activation barriers of rate-controlled step. By comparison the activation barriers of rate-controlled step, we conclude that among all CH_x(x = 1-3) species, CH_2 and CH_3 are the most favored monomer. In addition, the formation of CH_3OH is also investigated, suggesting that the formations of CH_2, CH_3 and CH_3OH by CO hydrogenation compete with each other on Cu(111) surface.

Acknowledgments

The work is supported financially by the National Natural Science Younger Foundation of China (No. 20906066), and the National Natural Science Foundation of China (No. 21276003, and 21276171).

References

[1] M.L. Poutsma, L.F. Elek, P.A. Ibarbia, A.P. Risch, J.A. Rabo, Journal of Catalysis 52 (1978) 157–168.
[2] J. Nerlov, I. Chorkendorff, Catalysis Letters 54 (1998) 171–176.
[3] J. Nerlov, S. Sckerl, J. Wambach, I. Chorkendorff, Applied Catalysis A-General 191 (2000) 97–109.
[4] M. Gupta, M.L. Smith, J.J. Spivey, ACS Catalysis 1 (2011) 641–656.
[5] J.J. Spivey, A. Egbebi, Chemical Society Reviews 36 (2007) 1514–1528.
[6] V. Subramani, S.K. Gangwal, Energy & Fuels 22 (2008) 814–839.
[7] M. Behrens, F. Studt, I. Kasatkin, S. Kühl, M. Hävecker, F. Abild-Pedersen, S. Zander, F. Girgsdies, P. Kurr, B.L. Kniep, M. Tovar, R.W. Fischer, J.K. Nørskov, R. Schlögl, Science 336 (2012) 893–897.
[8] J. Nerlov, I. Chorkendorff, Journal of Catalysis 181 (1999) 271–279.
[9] J. Szanyi, D.W. Goodman, Catalysis Letters 10 (1991) 383–390.
[10] Y. Choi, P. Liu, Journal of the American Chemical Society 131 (2009) 13054–13061.
[11] D. Mei, R. Rousseau, S.M. Kathmann, V.A. Glezakou, M.H. Engelhard, W. Jiang, C. Wang, M.A. Gerber, J.F. White, D.J. Stevens, Journal of Catalysis 271 (2010) 325–342.
[12] L. Han, D. Mao, J. Yu, Q. Guo, G. Lu, Catalysis Communications 23 (2012) 20–24.
[13] J.C. Slaa, J.G. van Ommen, J.R.H. Ross, Catalysis Today 15 (1992) 129–148.
[14] R. Xu, W. Wei, W.H. Li, T.D. Hu, Y.H. Sun, Journal of Molecular Catalysis A: Chemical 234 (2005) 75–83.
[15] R. Xu, C. Yang, W. Wei, W. Li, Y. Sun, T. Hu, Journal of Molecular Catalysis A: Chemical 221 (2004) 51–58.
[16] N. Zhao, R. Xu, W. Wei, Y. Sun, Reaction Kinetics and Catalysis Letters 75 (2002) 297–304.
[17] V. Mahdavi, M.H. Peyrovi, M. Islami, J.Y. Mehr, Applied Catalysis A: General 281 (2005) 259–265.
[18] C.E. Hofstadt, M. Schneider, O. Bock, K. Kochloefl, Studies of Surface Science and Catalysis, Preparation of Catalysis III 16 (1983) 709–721.

[19] S. Nave, A.K., Tiwari, B. Jackson, Journal of Chemical Physics 132 (2010) 054705-1–054705-12.
[20] Y. Pan, C. Liu, T.S. Wiltowski, Q. Ge, Catalysis Today 147 (2009) 68–76.
[21] P.W. van Grootel, E.J.M. Hensen, R.A. van Santen, Surface Science 603 (2009) 3275–3281.
[22] C. Michel, F. Auneau, F. Delbecq, P. Sautet, ACS Catalysis 1 (2011) 1430–1440.
[23] S. Lin, D. Xie, H. Guo, Journal of Physical Chemistry C 115 (2011) 20583–20589.
[24] P.W. van Grootel, E.J.M. Hensen, R.A. van Santen, Langmuir 26 (2010) 16339–16348.
[25] P. Rochana, J. Wilcox, Surface Science 605 (2011) 681–688.
[26] F. Fouda-Onana, O. Savadogo, Electrochimica Acta 54 (2009) 1769–1776.
[27] I.M. Ciobica, A.W. Kleyn, R.A. Van Santen, Journal of Physical Chemistry B 107 (2003) 164–172.
[28] Y. Yang, M.G. White, P. Liu, Journal of Physical Chemistry C 116 (2012) 248–256.
[29] L.C. Grabow, M. Mavrikakis, ACS Catalysis 1 (2011) 365–384.
[30] R.G. Zhang, H.Y. Liu, B.J. Wang, L.X. Ling, Journal of Physical Chemistry C 116 (2012) 22266–22280.
[31] Y. Yang, J. Evans, J.A. Rodriguez, M.G. Whiteac, P. Liu, Physical Chemistry Chemical Physics 12 (2010) 9909–9917.
[32] S.G. Wang, D.B. Cao, Y.W. Li, J. Wang, H. Jiao, Surface Science 603 (2009) 2600–2606.
[33] J. Greeley, M. Mavrikakis, Journal of the American Chemical Society 124 (2002) 7193–7201.
[34] B. Martorell, A. Clotet, Journal of Physical Chemistry C 113 (2009) 950–964.
[35] G. Kresse, D. Joubert, Physical Review B 59 (1999) 1758–1775.
[36] G. Kresse, J. Hafner, Physical Review B 47 (1993) 558–561.
[37] G. Kresse, J. Furthmuller, Physical Review B 54 (1996) 11169–21118.
[38] G. Kresse, J. Furthmuller, Computation Materials Science 6 (1996) 15–50.
[39] J.P. Perdew, J.A. Chevary, S.H. Vosko, K.A. Jackson, M.R. Pederson, D.J. Singh, C. Fiolhais, Physical Review B 46 (1992) 6671–6687.
[40] H.J. Monkhorst, J.D. Pack, Physical Review B 13 (1976) 5188–5192.
[41] M. Methfessel, A.T. Paxton, Physical Review B 40 (1989) 3616–3621.
[42] D. Sheppard, P., Xiao, W., Chemelewski, D.D., Johnson, G. Henkelman, Journal of Chemical Physics 136 (2012) 074103-1–8.
[43] D. Sheppard, R. Terrell, G. Henkelman, Journal of Chemical Physics 128 (2008) 134106-1–134106-10.
[44] G. Henkelman, H. Jónsson, Journal of Chemical Physics 111 (1999) 7010–7022.
[45] R.A. Olsen, G.J. Kroes, G. Henkelman, A. Arnaldsson, H. Jónsson, Journal of Chemical Physics 121 (2004) 9776–9792.
[46] X.K. Gu, W.X. Li, Journal of Physical Chemistry C 114 (2010) 21539–21547.
[47] W. An, X.C. Zeng, C.H. Turner, Journal of Chemical Physics 131 (2009) 174702-1–174702-11.